



MATHEMATICAL MODELING OF A FLAT PLATE SOLAR COLLECTOR WITH EUTECTIC SALTS AS PHASE CHANGE MATERIAL

O. F. Isamotu,* N. A. Musa, O. J. Okegbile, M. A. Orirafo and A. O. Bakare

(Mechanical Engineering, Engineering, Federal University of Technology, Minna, Nigeria)

*Corresponding author's email address: olakunleisamot@yahoo.com

ARTICLE INFORMATION

Submitted 18 Dec., 2020

Revised 19 April, 2020

Accepted 26 April, 2020

Keywords:

Thermal storage
solar collector
numerical model
phase change material
experimental validation

ABSTRACT

Solar energy is the most promising heat source for meeting energy demand without having negative impact on the environment. Solar energy is, however, intermittent in nature and time dependent energy source. In order to mitigate the intermittent supply of solar energy for water heating, the use of phase change material (PCM) comes into play. The PCM acts as a heat source for the solar heating system when the intensity of the solar radiation is low or no longer active. Knowledge about the thermal effectiveness of solar collector with PCM is paramount. So, this study developed a mathematical model to evaluate the thermal behavior of a flat plate solar collector integrated with a phase change material (PCM). This mathematical model developed for the flat-plate with PCM was based upon the conservation and heat transfer equations and used to predict the thermal behavior of integrated phase change material in solar collector during thermal storage. The energy balance equations for the flat-plate heating components of the collector and PCM were formulated numerically. The model was used to investigate the effect of inlet water temperature, water mass flow rate, outlet water temperature and the melt fraction during charging and discharging modes at each of the respective nodes. A comparison was made with a collector with and without PCM. The results show that charging and discharging processes of PCM have multiple stages. The addition of PCM in the first stage causes a decrease in temperature during charging and an increase during discharging. The highest water temperatures reached for the collector without and with a phase change material were approximately 51 and 74°C respectively. Comparisons were also made between the simulated and experimental data for the solar water heater without and with PCM. Minimum inlet water temperatures of 41.54 and 36°C were observed for the simulated and experimental model while, 42.69 and 74°C were both recorded for outlet temperatures respectively, for solar water heater without PCM. For the solar water heater with PCM, the inlet temperatures for the simulation and experimental model were found to be 42°C and 56°C respectively. A maximum outlet water temperature of 108°C was obtained from the experimental model compared to 45°C obtained from simulation. The temperature of the hot water obtained was remarkable and sufficiently enough for many domestic and industrial applications. Finally, the solar water heating system with phase change materials finds useful application and acts as a renewable energy resource in regions where there is inconsistent or poor sunlight.

© 2020 Faculty of Engineering, University of Maiduguri, Nigeria. All rights reserved.

1.0 Introduction

The growing number of problems with the world's dependence on fossil fuels continues to foster the public's desire to pursue clean, renewable sources of energy. Due to environmental issues and limited fossil fuel resources, more priorities are being given to renewable energy sources (Goswami, 2004). The energy from the sun is one form of renewable energy sources. It can be used for water heating in hot water systems, swimming pools as well as a supporting energy sources for central heating installations. The energy from the solar radiation is used for aforementioned purposes via solar collectors. At present the most often used solar collectors are liquid flat-plate collectors working either in parallel or perpendicular tube arrangement as well as the vacuum based structures. The flat plate collector supplies heat below 80°C when not integrated with phase change materials for energy storage and conservation (Hassan, 2003),

in reality, the indicative temperature range of operating fluid in flat plate collectors is between the range of 30-65°C (Kalogirou, 2004) and the system has an efficiency index higher than 0.5 typical for available flat plate collectors. Several studies have been carried out on the use of solar energy for heating purpose (Badescu, 2007). Notably, Nahar (2002) carried out studies on a solar water heater storage collector system and discovered that the system could generate about 50.6°C water at 4:00pm and 41.6°C water the next day with overall efficiency of about 47%. Similarly, Zerrouki et al. (2012), worked on a solar storage collector system in Algeria. The system achieved a maximum temperature of 53°C with an initial temperature of 17°C around 7:00am. A maximum flow rate occurred around 1:00pm. Kürklü et al. (2002), investigated a technique that could enhance the thermal performance of a flat-plate solar collector. It was found that the proposed design significantly improved the collector heat transfer characteristics in term of absorptivity and heat transfer coefficient. Rabin et al. (1995) developed a mathematical and experimental model for the charging process of a solar collector storage system, integrated with salt hydrate as a PCM. The proposed model showed high accurate validation with the experimental PCM temperature measurements. However, the neglect of the convection heat transfer in the stationary heat transfer reduced the accuracy of their mathematical predictions. Lin et al. (2012), proposed a comparative experimental study, under a typical sunny day in Malaysia, to investigate the possibility of enhancing the performance of a flat-plate solar collector by integrating paraffin wax with a melting temperature of 60.45°C directly in contact with the collector's absorber plate. The proposed collector achieved an efficiency of 52% at an inclination angle of 100, which was better by 23% than the conventional collector. Naghavi et al. (2015), proposed a theoretical model based on a one phase Stefan problem to investigate the thermal performance of integrating PCM to the manifold of an evacuated tube heat pipe solar collector system. It was revealed that the hot water volume and thermal efficiency of the baseline system significantly decreased with increase in the water volume flow rate from 50 to 80 litres per hour. The usable volume and the thermal efficiency almost remain the same in the innovative system.

Although a lot of work has been done on solar water heater (Lin et al, 2012) the need to devise a means of obtaining optimum performance of flat plate solar collector cannot be overemphasised. In view of this, Isamotu (2019) developed four different types of eutectic salt mixtures and found that the mixture of 1.77g of LiNO₃, 2.94g of NH₄NO₃, 1g of NaNO₃ and 1g of NaCl with melting point of 84.4°C and latent heat of 119KJ/Kg has better energy storage capabilities.

Therefore the aim of this work is to develop a mathematical model for solar collector with the eutectic salt mixture according to Isamotu (2019) as PCM

2.0 Materials and Method

The following materials were used in this research work: fiber glass, glass cover, absorber, working fluid, pipes (headers/risers), PCM, XMI400 solar dual transmission meter and KM250 thermocouple

2.1 Description of the Flat Plate Collector System

A flat plate collector consisting of a transparent cover, fluid, heat insulation, phase change materials, absorber plate, and collector casing were used. Figure 1 shows how the flat plate collector look likes. In line with the principle of operation, the sunlight passing through the glazing cover strikes the absorber plate and the solar radiation is converted into usable heat and transferred via its inner surface to the fluid passing through the respective nodes of the collector. Subsequently, the fluid carries the energy away from the collector for direct use or storage. The absorber plate is made of a thin (flat or grooved) high thermal conductivity metal sheet which could be steel, aluminum or copper. In order to maximize the efficiency of a solar collector, the surface of the absorber plate is painted with black colour pigment because of its high absorptivity property. The flow tubes in the collector are the integral parts of the absorber plate and these tubes are connected to the header tubes at both ends and either of

which could serve as a supply or return pipe (inlet, outlet). Some of the thermal energy is transferred via convection to the transfer fluid and the other is transferred by both conduction and convection to the phase change material beneath the absorber. When the absorbed temperature of the flat plate collector becomes higher than that of the PCM, the heat is first stored as a sensible heat until the PCM reaches its melting temperature. At this point, the PCM starts to melt and after complete melting, the released heat is stored back in the molten PCM as a sensible heat. When the sun was no longer active, all the solar components starts to cool down and the PCM at this point serves as the main heat source for the flat plate solar system.

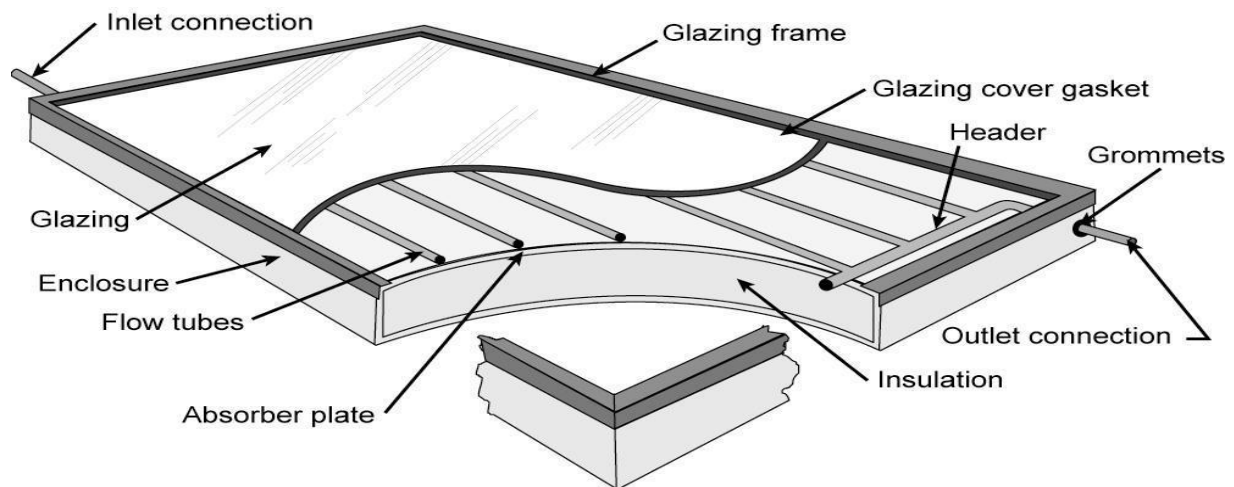


Figure 1: Cross sections of a flat plate collector (Alternative Energy Tutorials, 2012)

2.2 Mathematical model of a Flat plate collector with PCM

A schematic system study is depicted in Figure 2.

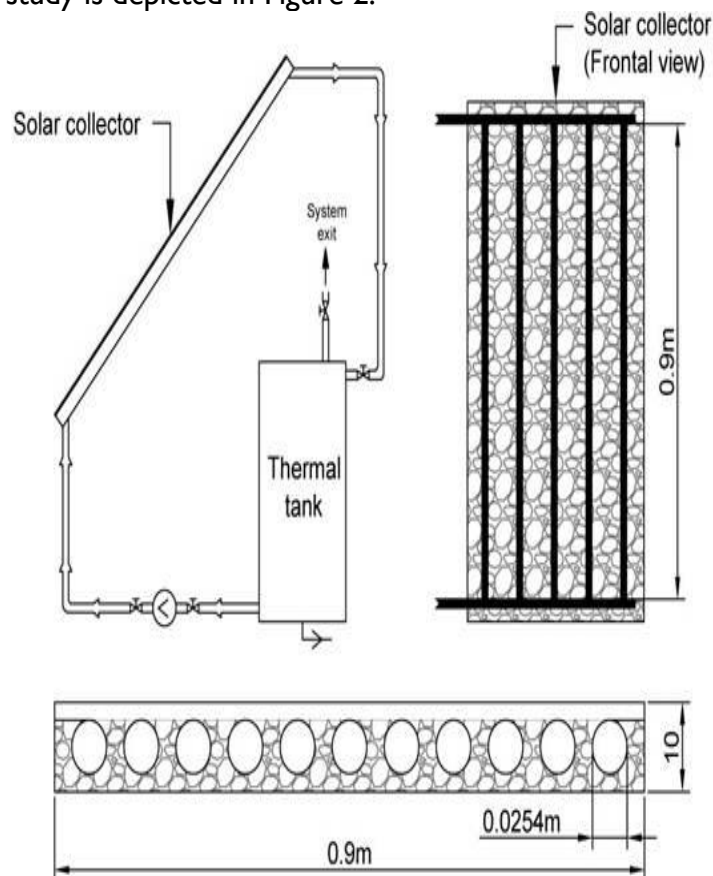


Figure 2: Schematic of a solar thermal system and setup (Badescu, 2007)

The system consists of a thermal solar panel, thermal tank, eutectic phase change materials, piping as well as control valves. The PCM (eutectic salt mixture) used in this system has a good thermal energy storage density and low thermal conductivity.

The PCM was then embedded in black colour pigment and used to coat the solar panel which was integrated into the heat-exchanger in the solar collector as shown in Figure 3.

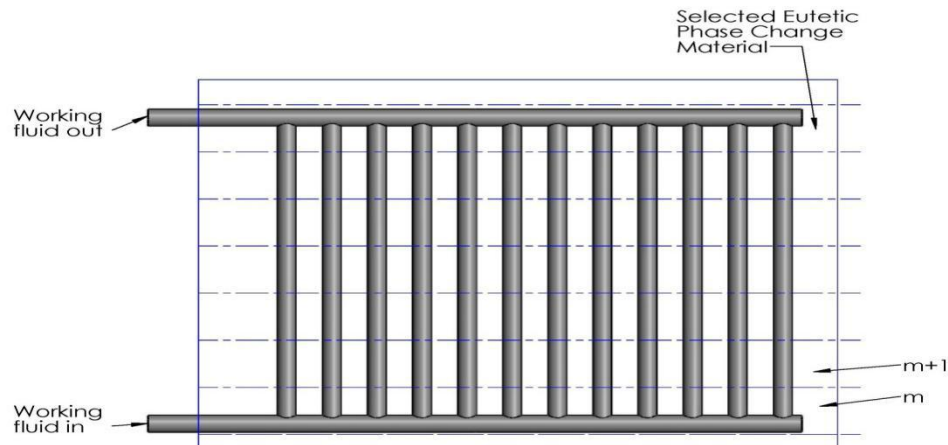


Figure 3: Solar tube heat exchanger finite-difference formulation (Badescu, 2007)

In order to write the energy conservation and heat transfer equations of the eutectic salt, the heat exchanger should be considered at each of the respective node because of the non-uniformly temperature distribution across each section. However, the model proposed is based on the following seven assumptions:

- (i) The thermo-physical properties of the PCM are independent of temperature, but different for solid and liquid phases.
- (ii) The heat transfer fluid is incompressible and it can be considered as a Newtonian fluid.
- (iii) The PCM is in perfect contact with the absorber.
- (iv) The PCM is homogeneous and isotropic.
- (v) The inlet velocity and inlet temperature of the heat transfer fluid are constant.
- (vi) No thermal expansion during melting process and
- (vii) The heat transfer in the direction of the transfer fluid is ignored.

The mathematical modeling of the heat transfer processes of a flat plate solar collector with PCM consist of both the solar radiation which is the source of the solar energy and the solar collector. The solar collector is further divided into seven sections has follows: The glass cover, absorber plate, air gap, transfer fluid, collector efficiency factor, collector heat removal factor and phase change materials.

Some of the mention parameters will be discussed individually,

Global solar radiation is the total amount of solar energy received by the earth's surface, usually expressed as W/m^2 . About 99 percent of global solar radiation has wavelengths between 300 and 3000 nm. This includes ultraviolet (300-400 nm), visible (400-700 nm), and infrared (700-3000 nm) radiation. Bekkouche(2008) proposed a theoretical model based on the following correlations. The solar irradiance are calculated as follows:

$$I = A \cos(\theta_1) \exp\left(-\frac{1}{B \sin(h+2)}\right) \quad (1)$$

where: h is the sun's height and θ_1 is the direct incident angle.

The diffuse irradiance is expressed as

$$D = \left(\frac{1 + \cos \beta}{2} \right) D_h = \left(\frac{1 - \cos \beta}{2} \right) \rho G_h \quad (2)$$

where: β the tilt is angle of the collector and ρ is the albedo
 D_h and ρG_h are further expressed as:

$$D_h = A'(\sin(h))^{0.4} \quad (3)$$

$$G_h = A''(\sin(h))^{B''} \quad (4)$$

The constants B, A', A'' and B'' depends on atmospheric state with time.

The energy balance equations for all of the seven components of the solar collectors mentioned earlier with temperature dependent is obtained for each of the components.

i. Glass covering

According to Zueva and Magiera (2001) the glass covering can be thus be written as:

$$c_g \rho_g V_g \frac{dT_g}{dt} = (h_{g,am}(T_{am} - T_g) + h_{r1}(T_{ab} - T_g) + h_{c1}(T_a - T_g) + \alpha G)p \nabla Z \quad (5)$$

where:

c = specific heat, ρ = density, V = volume, T = temperature, t = time, h = heat transfer coefficient, α = absorption coefficient, G = heat flux of solar radiation, p = tube pitch, Δz = spatial size of control volume

Subscripts notation: am = ambient, g = glass cover, a = air gap, ab = absorber, r = radiation c = convection

According to Duffie and Beckman (1974) the heat transfer coefficients by convection are calculated respectively as:

$$h_{cv,am} = 3.9v_{wind} + 5.62 \quad (6)$$

$$h_{cv,a} = \frac{Nu \lambda_a}{e_a} \quad (7)$$

v_{wind} , λ_a , e_a are the wind velocity, air thermal conductivity and the air gap thickness respectively.

The Nusselt number is calculated as follows:

$$Nu = (0.06 - 0.017 \left(\frac{\beta}{90} \right)) Gr^{0.33} \quad (8)$$

Gr is the Grashof number expressed as:

$$Gr = g \left(\frac{(T_{abs} - T_c) e_a^3}{\nu^2 T_a} \right) \quad (9)$$

The heat transfer coefficient by radiation is expressed as:

$$h_{r,c-as} = \epsilon_c \sigma (T_c^2 + T_{as}^2)(T_c + T_{as}) \quad (10)$$

where: T_{as} is the temperature of the air-space

The heat transfer coefficient by radiation on the absorber is expressed as:

$$h_{r,c-ab} = \sigma \left(\frac{(T_c^2 + T_{ab}^2)(T_c + T_{ab})}{\frac{1}{\epsilon_c} + \frac{1}{\epsilon_{ab}}} \right) \quad (11)$$

According to Duffie and Beckman (1974) T_{as} is expressed as:

$$T_{as} = 0.0553T_{am}^{\frac{3}{2}} \quad (12)$$

ii. The absorber plate

According to Shiv et al. (2010), the transient thermo-physical properties of the absorber material are considered when a heat energy balance is applied to the absorber zone. The solar irradiance on the absorber zone of the solar collector control volume, the radiation between the absorber and the glass cover, the conduction between the absorber and the insulation zone and the heat transfers by convection with the fluid flow need to be considered.

The following relation gives:

$$c_{ab}(T_{ab})\rho_{ab}(T_{ab})V_{ab} \frac{dT_{ab}}{dt} = \{G(\tau_a) + h_{r1}(T_{g-} - T_{ab}) + h_{c1}(T_a - T_{ab}) + \frac{k_i}{\delta_i}(T_i - T_{ab})\}p\Delta Z + \pi d_{in} h_f \Delta Z (T_f - T_{ab}) \quad (13)$$

where:

(τ_a) = Effective transmittance absorption coefficient, k = thermal conductivity, δ = thickness, d = diameter,

Subscripts:

i = insulation, f = working fluid, in = inner.

iii. Air gap of the flat plate collector

$$\rho_a V_a C_a \frac{dT_a}{dt} = h_{cv,c-a} S_c (T_c - T_a) + h_{cv,ab-a} S_{ab} (T_{ab} - T_a) + U_{loss,e} S_{a,e} (T_{am} - T_a) \quad (14)$$

According to Ahmad (2012), the heat exchange coefficient by convection can be estimated using (7)

$$Nu = 0.023Re^{0.8}Pr^{0.4} \quad (15)$$

Based on Incropera et al. (2006), the bottom loss and side loss coefficient of the collector is given as:

$$U_{loss,b} = \left(\frac{1}{\frac{\epsilon_{ins,b}}{\lambda_{ins,b}} + \frac{1}{h_{cv,wind}}} \right), U_{loss,s} = \left(\frac{1}{\frac{\epsilon_{ins,s}}{\lambda_{ins,s}} + \frac{1}{h_{cv,wind}}} \right) \quad (16)$$

The thermal heat exchange with the phase change materials during charging and discharging modes are expressed as follows:

$$Q_{ab,PCM} = -\lambda_{PCM,i} S_{PCM} \frac{\delta T_{PCM,i}}{\delta x} \quad (17)$$

$$Q_{ab,PCM} = \lambda_{PCM,i} S_{PCM} \frac{\delta T_{PCM,i}}{\delta x} \quad (18)$$

where: $i = \text{solid}$ when the phase change material is in the solid state and $i = \text{liquid}$ when the phase change material is in the liquid state.

iv. Heat transfer fluid

According to Klein et al. (1974), the heat exchange coefficient of the collector can be determine as putting the tube cross section of the solar collector into consideration A_{htf} the conservation energy equation for the HTF becomes

$$\rho_{htf} C_{htf} \frac{\partial T_{htf}}{\partial t} = - \frac{c_{htf} \dot{m}_{htf}}{A_{htf}} \frac{\partial T_{htf}}{\partial x} + \frac{h \pi D_i}{A_{htf}} (T_w - T_{htf}) \quad (19)$$

The thermal resistance of the wall is assumed to be negligible, the conservation energy equation of the wall now becomes:

$$\rho_w C_w \frac{\partial T_w}{\partial t} = \frac{h \pi D}{A_w} (T_{htf} - T_w) + \frac{1}{s_w} \left(\frac{k_w A_w^1}{A_w} + \frac{k_{pcm} A_{pcm}^1}{A_w} \right) (T_{pcm} - T_w) \quad (20)$$

where:

A_w = Cross sectional area of the wall

k_w and k_{pcm} are the thermal conductivity of the wall and the PCM respectively

The heat transfer conduction within the PCM in the axial direction is negligible, therefore the conservation energy equation in the first cell of the PCM alternate to the wall becomes:

$$\rho_{pcm} \frac{\partial H_{pcm}}{\partial t} = \frac{1}{s_w} \left(\frac{k_w A_w^1}{A_w} + \frac{k_{pcm} A_{pcm}^1}{A_w} \right) (T_{pcm} - T_w) + \frac{1}{s_w} \frac{k_{pcm}}{A_{pcm}} \left(\frac{H_{pcm}^{j+1}}{A_w} - \frac{H_{pcm}^j}{A_w} \right) \quad (21)$$

The energy conservation equation for the generic cell of the PCM becomes:

$$\rho_{pcm} \frac{\partial H_{pcm}}{\partial t} = \frac{k_{pcm}}{c_{pcm}} \left(\frac{1}{r} \frac{\partial}{\partial r} \left(r \frac{\partial H_{pcm}}{\partial r} \right) \right) \quad (22)$$

Charging phase: During this phase the water mass flow rate can be calculated from the heat released through solar radiation.

Mass flow rate of water is expressed as:

$$m_w = \frac{G A_{collectors}}{1000 \times C_{pw} \times \Delta T_w \times n} \quad (23)$$

where: m_w , Water mass flow rate $\left(\frac{kg}{s} \right)$, G , Radiation $\left(\frac{W}{m^2} \right)$, A , Area of the collector (m^2),

C_{pw} , Specific heat of water $\left(\frac{kJ}{kgK} \right)$, ΔT_w , The heat transfer fluid temperature difference, n , number of tubes in the solar collector.

According to Laouadi and Lacroix, (1999) the finite-difference formulation of the time derivative can be written for the solid phase as follows;

Solid phase:

$$T_{PCM_{m+1}} = T_{PCM_m} + \frac{m_w C_{pw} \Delta T_w}{\rho_s V_{PCM} C_{ps}} \Delta t \quad (24)$$

where: T_{PCM_m} , Temperature of PCM at m element ($^{\circ}C$), ρ_s , Density of PCM at solid phase ($\frac{kg}{m^3}$), V_{PCM} , PCM volume (m^3) C_{p_s} , PCM specific heat at solid phase ($\frac{kJ}{kgK}$), Δt , time differential (s).

The same finite-difference formulation of the time derivative can be applied to the mushy and liquid phase as follows;

$$\gamma_{m+1} = \gamma_m + \frac{m_w c_{pw} \Delta T_{w,mushy}}{\rho_L V_{PCM} h_L} \Delta t \quad (25)$$

Heat along the tubes of the collector according to Senthilkumar et al. (2014) is expressed as

$$Q_{tube} = \rho_L V_{PCM} h_L \gamma \Delta t \quad (26)$$

where: γ_m , Liquid fraction at element h_L , PCM latent heat ($\frac{kJ}{kg}$), ρ_L , Density of PCM at liquid phase ($\frac{kg}{m^3}$), Q_{tube} , Heat along each tube (kJ),

The finite-difference formulation of the time derivative can be applied to the liquid PCM as follows;

$$T_{PCM_{m+1}} = T_{PCM_m} + \frac{m_w c_{pw} \Delta T_w}{\rho_L V_{PCM} C_{pL}} \Delta t \quad (27)$$

Discharging phase

This is the stage when the phase change material experiences phase change from liquid to mushy and solid. The rate of useful energy gain in this stage is less than the rate of the thermal losses at the point where the PCM starts to solidify. The water mass flow rate of heat transfer fluid during the discharge process can be calculated as follows;

$$m_w = \frac{Q_{charging}}{C_{pw} \times \Delta T_w \times n} \quad (28)$$

The total heat absorbed during the charging phase by the phase change materials in all of the three stages is expressed as:

$$Q_{charging} = m_{PCM} (C_{p_s} \Delta T_s + h_L + C_{p_L} \Delta T_L) \times n \quad (29)$$

where: m_{PCM} , is the mass of the phase change material per finite different element.

2.3 Experimental evaluation of the solar water heater with PCM based thermal storage

The experimental setup of the solar water heater with PCM based thermal storage is shown in Figure 4.



Figure 4: The Experimental setup of a solar water heater with PCM

The experiments were carried out between the hours of 9:00AM and 20:00 PM every day for four consecutive days and the temperatures of the storage at every 6:30AM were carefully observed. The flow rate of the water was controlled and manipulated by a water regulator. Solar intensity was measured by solar dual transmission meter XMI400 (manufactured in USA by EDTM INC). The temperatures at the different points (inlet, outlet, glass, absorber, and storage tank) of the system were measured by digital thermocouples KM 250 (manufactured in Australia by ACKSEN INC.).

3. Results and Discussion

The systems of Equation (1) through (29) has been numerically solved using the finite difference scheme for the adopted phase change materials (eutectic metallic salts) and the results shown in Figures 5 to 8 Global, ambient condition, glass condition, water inlet conditions, heat transfer fluid temperature with respect to time, solar insolation, and water outlet condition are shown in Figures 5 to 8

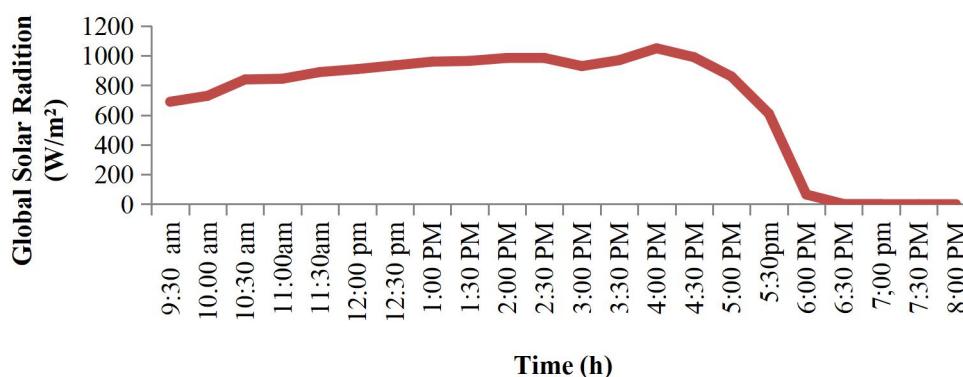


Figure 5: Global solar radiation against time

Figure 5 presents the time variation of solar insolation (W/m²) measured at the site where the research was conducted. It is clear that the intensity of radiation depends upon the hour of the

day and the period of the year. Additionally, it can be deduced that the solar irradiance at 9:30 Am was observed to be 690W/m^2 and the intensity kept on increasing with time until it reaches its peak at 4:00 pm. At this time 1050W/m^2 was recorded which can be said to be progressive with respect to the result obtained in heating the water. The solar intensity declined from the peak value of 1050W/m^2 in the hour of 4.00pm to 0W/m^2 in the hours of 6.30, 7.00, 7.30 and 8.00pm as evident in Figure 5.

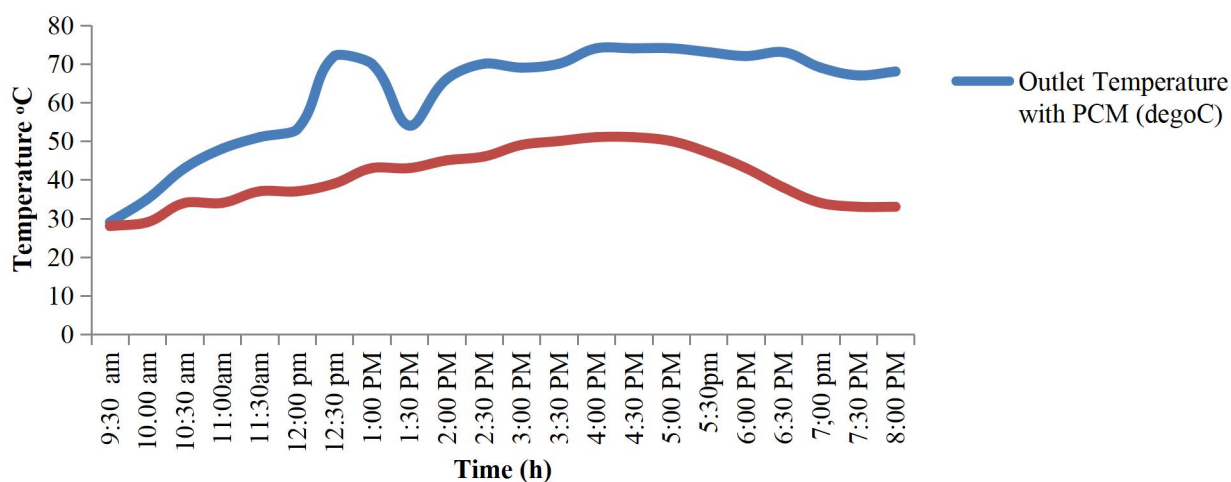


Figure 6: Hourly variations of outlet water temperature without and with PCM

Figure 6 shows the temperature variations of outlet water temperature without and with PCM as a function of time. For both cases, the temperatures increased with time till it reached maximum values and then gradually decreased. The highest water temperatures reached for the collector without and with a phase change material were approximately 51 and 74°C respectively. This was as a result of the rise of solar intensity experienced during that day till 4.30 pm. It was observed that for the case without PCM, all the absorbed solar radiations were used to heat the transfer fluid, contrary to the case where the PCM was used.

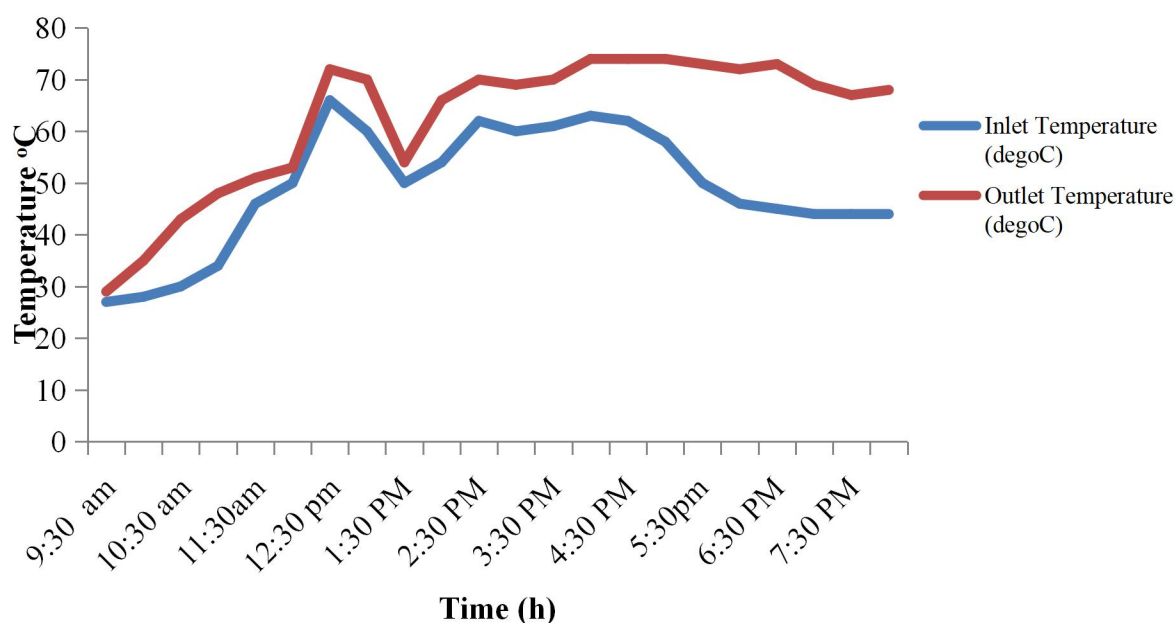


Figure 7: Effect of inlet temperature on outlet water temperature

The effect of inlet water temperature on its outlet temperature was shown in Figure 7. The maximum inlet temperature of 63°C was observed around 4 pm. The temperature however was not steady, it fluctuated upward and backward, as a result of non-uniform temperature

distribution at each of the respective nodes of the collector. An increase in inlet temperature led to a rise in outlet water temperature. A maximum steady temperature of 74°C was recorded at the outlet. The rise was mostly enhanced at higher inlet water temperature. Figure 8 shows the variation of ambient, water inlet, water outlet and glass temperatures with respect to time.

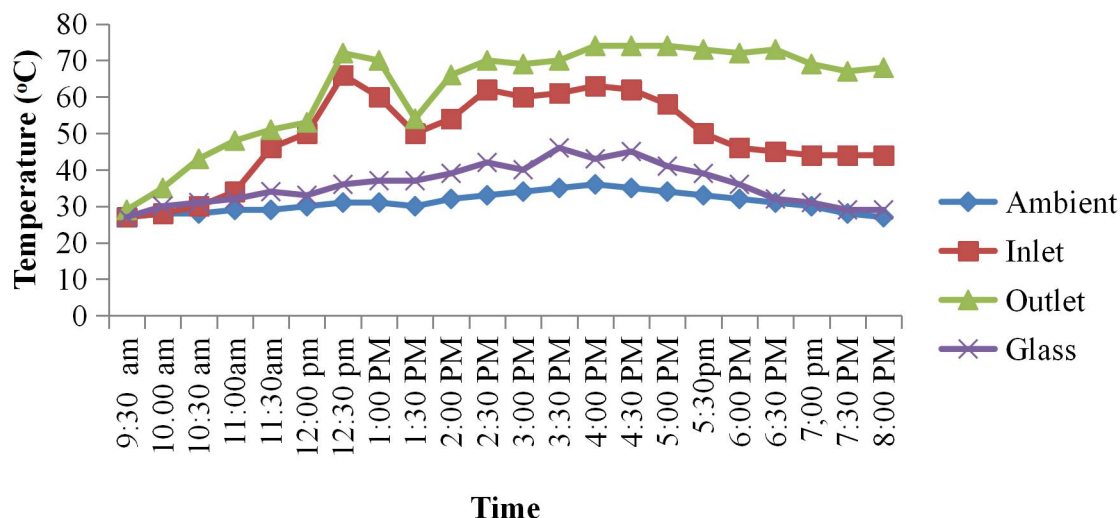


Figure 8: The variation of ambient, water inlet, water outlet and glass temperatures with time. It was clear that the inlet water temperature was 27°C at 9:30am in the morning which also corresponded to the ambient temperature and glass temperature at that point. Figure 8 showed that the outlet temperature increases with time. At about 12:30 pm a temperature of 66°C was recorded at the inlet and 72°C at outlet. The glass maintained a temperature of 36°C, while the ambient at this time was 31°C. The temperature of the glass is higher than that of ambient air because of the green house effect exhibited by it. The storage tank which houses the water has a temperature of 39°C at the upper layer and 30°C at the lower layer indicating a non-uniform temperature distribution in each of the layers. The thermal gradient curve of the graph clearly showed that the temperature rises with height which is the factor responsible for the hot water to stay above the cold water layer as a result of difference in density. The glass and ambient air reached their peak temperatures of 46°C and 36°C at 3.30pm and 4.00pm respectively. Maximum water outlet temperature of 74°C was obtained at 4.00pm and 5.00pm. At 8.00pm, when the solar energy was no longer accessible, the glass, ambient air and outlet water temperatures dropped to 29°C, 27°C and 68°C respectively as seen in Figure 8. Figure 9 was constructed to compare experimental result with simulation result.

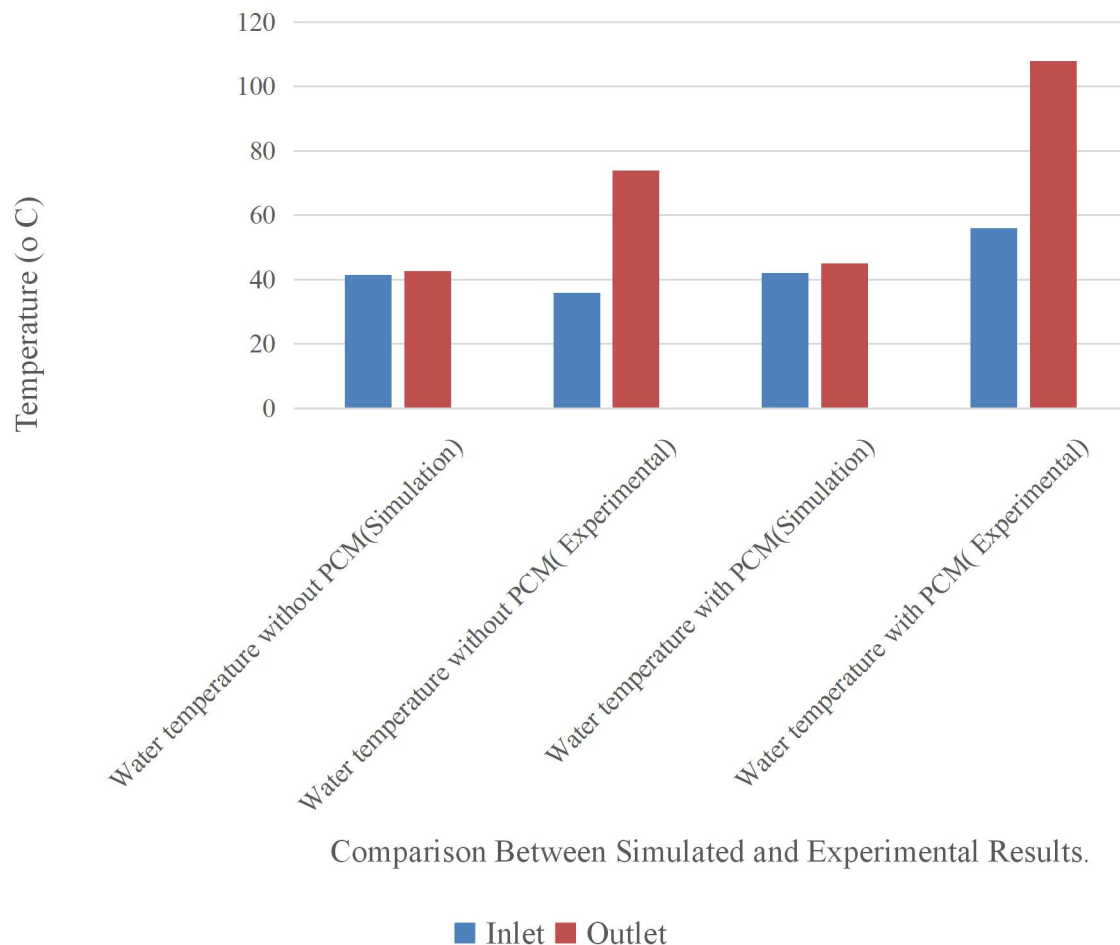


Figure 9: Comparison between the results obtained from simulation and experimental results

Temperature is the most significant parameter in the solar water heating system used in validating the experimental result. Figure 9 showed both the inlet and outlet water temperatures of the simulated model as well as the experimental for solar water heater without PCM and with PCM. Inlet temperatures of 41.54 and 36°C were observed for both the simulated and experimental model for the solar water heater without PCM, while 42.69 and 74°C were recorded for the outlet temperatures respectively. It was observed that the data of the outlet temperatures of the experimental model outweighed the outlet temperature of the simulated model. Additionally, the solar water heater with PCM, the inlet temperatures for the simulation and experimental model were found to be 42°C and 56°C respectively. A maximum outlet water temperature of 108°C was obtained from the experimental model and 45°C was obtained from simulation model. The result of the simulation model fairly agrees with the ones obtained by Nahar (2002) whose experiment generated a maximum output temperature of 50.6°C at the solar peak period and 41.6°C the next morning and Akuffo and Jackson, (2008) whose experiments generated a maximum outlet temperature of 45°C at solar peak period. The overall progression of the graph confirmed the efficiency and heat retaining capacity of the adopted phase change materials used in the research work.

4.0 Conclusion

A one dimensional theoretical model for a flat plate solar collector with phase change material was developed to investigate the thermal performance of the system. It is noteworthy that the numerical model presented, predicted the heat transfer characteristics during phase change material and interactions between the heat transfer fluids. The experimental data was also

validated with the numerical model and simulation. The results presented shows that the heat absorbed during the charging process increases at higher water mass flow rates and decreases during discharging process at higher water mass flow rates while the time needed to complete melting and solidification modes are not linear with the mass flow rate and the PCM. This research work indicated that salt hydrates are the most energy intensive of the PCM possibilities when compared to paraffin for energy storage. This assessment shows that when PCM was used as a medium for energy storage, it significantly accumulates more energy than when water was used as a medium for energy storage. The temperature of the hot water obtained was remarkable and sufficiently enough for many domestic and industrial applications. Finally, the solar water heating system with phase change materials finds useful application and acts as a renewable energy resource in regions where there is inconsistent or poor sunlight.

References

- Ahmad, MS. 2012. Modeling of flat plate solar collector operation in transient states. M.Sc. Thesis, Purdue University, U.S.A.
- Akuffo FO. and Jackson, EA. 2008. Simulation studies on a compact solar water heater in the tropics. *Solar and Wind Technology*, 5: 229-237.
- Alternative Energy Tutorials. 2012. Alternative and Renewable energy. Retrieved July 20, 2012 from <http://www.alternative-energy-tutorials.com/>
- Badescu, V. 2007. Optimal control of flow in solar collectors for maximum exergy extraction. *International Journal of Heat and Mass Transfer*, 50: 4311–4322.
- Bekkouche, SMA. 2008. Modélisation du comportement thermique de quelques dispositifs solaires. Ph.D Thesis, University Abou-bakar Belkaid- Tlemcen, Algeria.
- Duffie, JA., Beckman, WA. 1974. *Solar energy thermal process*, Wiley Interscience, New York.
- Goswami, DY., Vijayaraghavan, S., Lu, S. and Tamm, G. 2004. New and emerging developments in solar energy. *Solar Energy*, 76: 33-43.
- Hassan, MM. 2003. Framework for Evaluation of Active Solar Collection Systems. Ph.D. thesis, Virginia Polytechnic Institute and State University, Blacksburg, Virginia, USA.
- Incropera, FP., Dewitt, DP., Bergman, TL and Lavine, VS. 2006. *Fundamentals of heat and mass transfer*, Six edition, John Wiley and Sons, Hoboken, New Jersey, USA.
- Isamotu, OF. 2019. Development of solar water heater with phase change materials based thermal storage. M.Eng Thesis, Federal University of Technology, Minna, Niger State, Nigeria.
- Kalogirou, SA. 2004. Solar thermal collectors and applications. *Progress in Energy and Combustion Science*, 30: 231–295.
- Klein, S., Duffie, J. and Beckman, W. 1974. Transient considerations of flat-plate solar collectors, *Trans. of ASME: Journal Engineering for Power*, 96: 109-113.
- Kürklü, A., Özmerzi, A. and Bilgin, S. 2002. Thermal performance of water-phase change material solar collector. *Renewable Energy*, 26(3): 391–399.
- Laouadi, A. and Lacroix, M. 1999. Thermal performance of a latent heat energy storage ventilated panel for electric load management. *International Journal of Heat Mass Transfer*, 42: 275-286.
- Lin, SC., Al-kayiem, HH. and Aris, MS. 2012. Experimental investigation on the performance enhancement of integrated PCM-flat plate solar collector. *Journal of Applied Sciences*, 12(9): 2390–2396.

Naghavi, MS., Ong, KS., Badruddin, IA., Mehrali, M., Silakhori, M. and Metselaar, HSC. 2015. Theoretical model of an evacuated tube heat pipe solar collector integrated with phase change material. *Energy*, 91:911–924.

Nahar, NM. 2002. Capital cost and economic viability of thermosyphonic solar water heaters manufactured from alternate materials in India. *Renewable Energy*, 26: 623-635.

Rabin, Y., Bar-Niv, I., Korin, E. and Mikic, B. 1995. Integrated solar collector storage system based on a salt-hydrate phase change material. *Solar Energy*, 55: 435–444.

Senthilkumar, R., Sithivinayagam, N. and Shankar, N. 2014. Experimental investigation of solar water heater using phase change material. *International Journal of Research in Invent Technology*, 2(7): 1110-1117.

Shiv, K., Tiwari, GN. and Gaur, MK. 2010. Development of empirical relation to evaluate the heat transfer coefficients and fractional energy in basin type hybrid (PV/T) active solar still. *Desalination*, 250: 214-221.

Zerrouki, A., Boumedien, A. and Bouhadeif, K. 2012. The natural circulation solar water heater model with linear temperature distribution. *Renewable Energy*, 26: 549-559.

Zueva, G. and Magiera, J. 2001. Mathematical model of heat transfer in solar collector and its experimental validation. *Theoretical Foundations of Chemical Engineering*, (6): 604-608